Chem. Chem. Technol., 2023,
Vol. 17, No. 3, pp. 518–531

Chemistry

[3+2] CYCLOADDITION OF N-*TERT*-BUTYL,α-(4-TRIFLUOROMETHYL)-PHENYLNITRONE WITH METHACROLEIN: THEORETICAL INVESTIGATION

***Khaoula Kouchkar*[1], *Youcef Boumedjane*[1], *Salah Eddine Hachani*[2, ✉]**

https://doi.org/10.23939/chcht17.03.518

Abstract. In this scientific contribution, regio- and diastereo- selectivity of [3+2] cycloaddition (32CA) of N-*tert*-butyl,α-(4-trifluoromethyl)-phenylnitrone (**1**) with methacrolein (**2**) were investigated using DFT method at B3LYP/6-31(d) computational level in gas and dichloromethane solvent. The molecular electrostatic potential MESP was used to show the most active centers in the examined molecules. Global and local reactivity indices as well as thermodynamic parameters have been calculated to explain the regioselectivity and stereoselectivity for the selected reaction. The possible chemoselective *ortho*/*meta* regioselectivity and stereo- (*endo*/*exo*) isomeric channels were investigated. Our theoretical results give important elucidations for the possible pathways related to the studied 32CA reaction.

Keywords: [3+2] cycloaddition, N-*tert*-butyl,α-(4-trifluoromethyl)-phenyl, methacrolein, DFT, regioselectivity, stereoselectivity.

1. Introduction

Many chemical processes can be used to elaborate new heterocyclic molecular systems. The [3+2] cycloaddition (32CA) reaction between a three atom component (TAC) and a dipolarophile is a very useful synthetic method for the preparation of five-membered heterocyclic with multiple stereogenic centers, usually with excellent stereocontrol.[1,2]

The scientific papers have reported that the 32CA reactions should follow one of these mechanisms:

- Non-polar mechanisms (synchronical mechanism or stepwise, biradical mechanism) – an example of this type is the cycloaddition of (Z)-C, N-diphenylnitrone and 1,2-bismethylene-3,3,4,4,5,5 hexamethylcyclopentane, this reaction process occurs without the intervention of a biradical intermediate. In particular, these 32CA reactions proceed *via* a low polar one-step mechanism.[3]

- Polar mechanisms, such is confirmed by the recent comprehensive DFT studies,[4] for example [3+2] cycloaddition between (Z)-C-(3,4,5-trimethoxyphenyl)-N-methyl-nitrone and (Z)-2-EWG-1-bromo-1-nitroethenes. The formation of the isoxazolidine ring on all analyzed [3+2] cycloaddition pathways occurs in the toluene solution according to the one-step mechanism. When toluene is a replacement for the more polar nitromethane, the stepwise, zwitterionic mechanism is very possible.

Additionally, Radomir Jasinski,[5] has studied zwitterionic or biradical adducts between the nitroacetylene and allenyl-type TACs, DFT calculations for various theory levels show that [2+3] cycloaddition reactions take place according to the polar mechanism. This is not, however, the expected two-step, zwitterionic mechanism, but a one-step mechanism. Zwitterionic structures with the "extended" confirmation may theoretically form along competitive paths.

In the last decade, experimental studies based on the [3+2] cycloaddition between aryl-alkyl nitrones with π-deficient alkenes have been performed. In a study, reactions between nitroethene (1) and benzonitrile N-oxides (2) are giving high yields of 3-aryl-5-nitroisoxazolines (4) (see Scheme 1).[6]

Radomir Jasinski has computationally studied the 32CA of (Z)-C,N-diphenylnitrone with 1,1-dinitroethene leading to the formation the regioisomeric adducts: 2,3-diphenyl-5,5-dinitroisoxazolidine (**3**) and 2,3-diphenyl-4,4-dinitroisoxazolidine (**4**) heterocyclic ring (see Scheme 2). The theoretical data have revealed that the formation 2,3-diphenyl-4,4-dinitroisoxazolidine (**4**) was privileged, these results were in full agreement with the experimental observations earlier reported.[7]

The [3+2] cycloaddition generally gives two products with various proportions. In fact, the laboratory techniques cannot give further insights into the cycloaddition reactions. Besides, these experimental methods are expensive and time-consuming.

[1] Group of Computational and Pharmaceutical Chemistry, LMCE Laboratory, University of Biskra, BP 145 Biskra, 07000, Algeria
[2] University of Biskra, Laboratory of Applied Chemistry LCA, 07000, Biskra, Algeria
✉ *salaho_hachani@yahoo.fr*

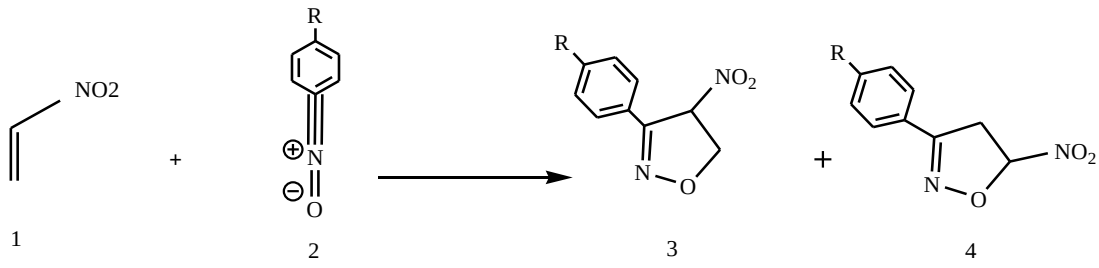

Scheme 1. 32CA between nitroethene (**1**) and benzonitrile N-oxides (**2**)

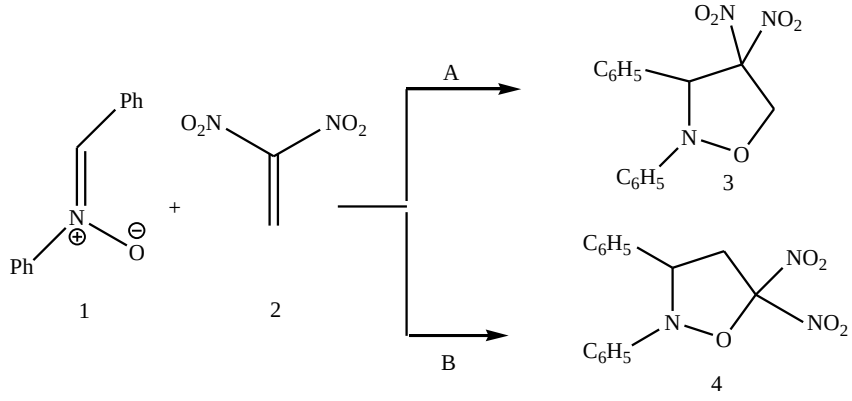

Scheme 2. 32CA of (Z)-C,N-diphenylnitrone (**1**) with 1,1-dinitroethene (**2**)

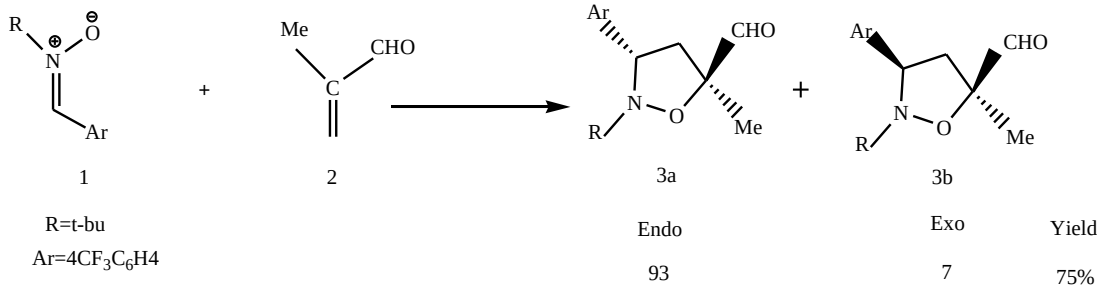

Scheme 3. 32CA of N-*tert*-butyl, α-(4-trifluoromethyl)-phenylnitrone (**1**) with methacrolein (**2**)

Computer development opens the door to scientists to use theoretical chemistry basics for deep understanding of the cycloaddition experimental results.[8-10] Density functional theory (DFT) approaches are used as a powerful tool to give quantum reactivity descriptors explored for the prediction of the regioselectivity and stereoselectivity in the cycloaddition process.[11]

Isoxazolidines compounds are formed by reacting alkenes and nitrones. These molecules have gained much attention in the field of organic chemistry due to their unique properties. These chemical species exhibit important biological activity.[12,13] The studies on isoxazolidines have reported that such kinds of compounds could be used as enzyme inhibitors.[14,15] The isoxalidines hold promise to be used in the treatment of HIV and cytotoxicity, arising from their ability to act as nucleoside analogs.[16-18] In addition, they have served as synthetic precursors to other classes of natural products, such as 1,3-amino alcohols, β-lactams, and alkaloids with physiological activity.[19-23]

In recent research, Badoiu and coworkers have processed cycloaddition between N-*tert*-butyl,α-(4-trifluoromethyl)-phenylnitrone (**1**) (α-arylnitrone 1) with methacrolein (**2**), they have reported that this reaction give preferentially two products namely 3a, 3b with the ratio of 93:7, yield 75 %, respectively (Scheme 3).[24] To the best of our knowledge, there is not any theoretical background treating the regio-, stereo-, and diastereo-selectivity of the above-mentioned reaction.

This work represents a theoretical study of the regio-, stereo-, and diastereo-selectivity of the products observed experimentally. Global reactivity indices includ-

ing the energies of the HOMO and LUMO molecular orbitals of each reagent, chemical hardness (η), electronic chemical potential (μ), global electrophilicity (ω), global nucleophilicity (*N*) as well as Wiberg bond indices, bond order, and charge transfer at the transition states have been calculated to bridge the gap between our theoretical data and the experimental results earlier reported.

2. Computational Details

The molecular structures of the reagents under investigations are built using Gauss View 6.0.8 and then fully frequency optimized using GAUSSIAN 09 program package[25] at DFT Beck Three Lee, Yang and Parr (B3LYP) functional combined with 6-31G(d) basis set level of theory.[26-28] All calculations have been performed in an organic solvent (dichloromethane) using self-consistent reaction field (SCRF)[29,30] associated with a polarizable continuum model (PCM).[31] This approach models dichloromethane (DCM) solvent as dielectric constant (ε=8.93).

The charge transfer or in the sense the global electron density transfer (GEDT)[32] and bond order (Wiberg indexes)[33] have been analyzed *via* the natural bond orbital (NBO) at full stationary point.[34-36] Analysis of the thermodynamic parameters, of the reaction α-arylnitrone 1 and methacrolein 2-*cis*/*trans* were realized using the MPW1PW91/6-31G(d) thermodynamic data, in dichloromethane at 298.150 K and 1 atm.[37] The intrinsic reaction coordinates (IRC analysis)[38] were also computed to analyze the studied mechanism in detail for all the obtained transition structures.

The global electrophilicity index (ω) corresponding to our dipole and dipolarophile is calculated by the following equation:[39]

$$\omega = (\mu^2/2\eta) \quad (1)$$

In Eq. (1), μ and η are the electronic chemical potential and the chemical hardness, respectively,[11,40] these quantum parameters can be calculated using the energies of the highest occupied molecular orbital ε_H and the lowest unoccupied molecular orbital ε_L using the following formulas:

$$\mu \approx (\varepsilon_H + \varepsilon_L) \quad (2)$$

$$\eta \approx (\varepsilon_L - \varepsilon_H) \quad (3)$$

The global nucleophilicity N[41] was calculated as follows:

$$N = E_{HOMO\ (nucleophile)} - E_{HOMO\ (TCE)} \quad (4)$$

In relation (4), $E_{HOMO\ (TCE)}$ is dedicated to the HOMO energy of tetracyanoethylene. In our case of study $E_{HOMO\ (TCE)}$ = -0.3352 a.u.

To analyze the selective sites in dipole and dipolarophile the local Fukui functions indices need to be defined. Thus, calculating Fukui functions helps us to determine the active sites of a molecule, based on the electronic density changes experienced by it during 32CA reaction.

For an atom *k* in a molecule, depending upon the type of electron transfer, we have two different types of condensed Fukui function of the atom *k*, which are calculated using the following equations:[42]

$$f^+ = [\rho_k (N + 1) - \rho_k (N)]$$
(for nucleophilic attack) (5)

$$f- = [\rho_k (N) - \rho_k (N - 1)]$$
(for electrophilic attack) (6)

where ρ_k (N), ρ_k (N-1), and ρ_k (N+1) are dedicated to the electronic populations of the site *k* in neutral, cationic, and anionic forms of the studied molecular system, respectively.

On the other hand, and in analogy to our global electrophilicity index (ω) and nucleophilicity index (*N*), we have also introduced the local electrophilicity (ω_k),[43] and local nucleophilicity (N_k),[44] through to the formulas:

$$\omega_k = \omega f_k^+ \quad (7)$$

$$N_k = N f_k^- \quad (8)$$

In turn, the σ bond development (l) indices were designated based on the formula:[45]

$$I_{X-Y} = 1 - \frac{r^{TS}_{X-Y} - r^{P}_{X-Y}}{r^{P}_{X-Y}} \quad (9)$$

3. Results and Discussion

3.1. Global Reactivity Indices of Reagents

Sustmann *et al.* have reported that the main interactions in cycloaddition could occur either between the E_{LUMO} of the dipole (nitrone) and the E_{HOMO} of dipolarophile (alkene), namely inverse electronic demand (IED) character, or between the E_{LUMO} of dipolarophile (alkene) and the E_{HOMO} of the dipole (nitrone), called normal electronic demand (NED) character.[46]

The electronic demand (NED) and inverse electronic demand (IED) characters related to the studied cycloaddition reaction has been evaluated using the energies E_{HOMO} and E_{LUMO} of the reactants according to the equation and listed in Table 1.

Table 1. NED and IED values calculated at DFT/B3LYP/6-31G(d) level of theory (eV)

IED	NED
5.28	4.06

It is apparent that the $|E_{LUMO}$ of dipolarophile – E_{HOMO} of dipole difference (4.06 eV) is smaller than the E_{LUMO} of dipole -E_{HOMO} of dipolarophile| one (5.28 eV), this theoretical result demonstrated that NED is the predominant character for our 32CA case of study.

In Table 2, we have reported the energies of the HOMO and LUMO molecular orbitals of each reagent, values of chemical hardness (η), electronic chemical potential (μ), global electrophilicity (ω), global nucleophilicity (*N*) are calculated at B3LYP/6-31G(d) level in the gas phase.

As can been seen from Table 2, the value of chemical potential (μ) of the dipole is bigger than that of dipolarophile, which indicates that the charge transfer or global electron density transfer (GEDT)[29] will go from 1, 3-dipole toward dipolarophile (NED: Normal Electronic Demand).

The global hardness is an important chemical parameter that measures the resistance of chemical species such as molecules towards electron cloud polarization or deformation generated during a chemical reaction. 32CA reaction is related to lower hardness and higher soft character of the reactants. The values of hardness and its reciprocal softness of the studied reactants are lower confirming that 32CA reaction could be possible.

The electrophilicity (ω) and the nucleophilicity (*N*) values to the dipole and dipolarophile displayed in Table 2 shows that the dipolarophile could act as a powerful electrophile and the dipole could behave as a strong nucleophile.

Molecular electrostatic potential surfaces MEPS proposed by Tomasi *et al.* can inform about the electronegative and the electropositive centers in the molecules of the reactants under probe.[47,48] Generally, the molecular regions having higher electronegativity are colored in red whereas the regions possessing higher electropositivity are depicted in blue. Regarding the MEPS of our reactants shown in Fig. 1, it can be seen that oxygen and fluorine atoms of the α-aryl nitrone and the oxygen atom of the methacrolein are of red color, which reveals that these atoms have a negative charge, hence the interactions between these atoms is impossible.

Electropositive regions (blue) around the C=C double bond of methacrolein indicate that the C=C double bond is very electrophile atoms. The most favorable interactions have occurred between the oxygen of α-aryl nitrone (**1**) and the C=C double bond of methacrolein (**2**).

Table 2. Global reactivity indices of the analyzed dipole and dipolarophile calculated at DFT/B3LYP/6-31G(d) level of theory

	E_{HOMO}	E_{LUMO}	μ (a.u)	η (a.u)	ω (eV)	N^a (eV)
Dipole	-0.2109	-0.0601	-0.1355	0.1508	1.6500	3.3700
Dipolarophile	-0.2551	-0.0611	-0.1581	0.1940	1.7500	2.1700

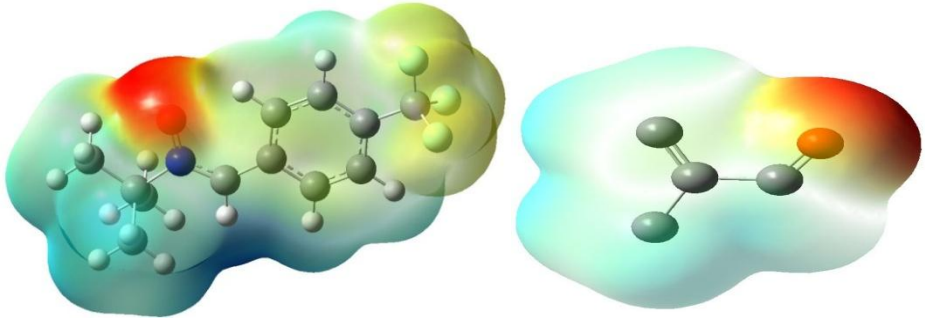

α-aryl nitrone (**1**) methacrolein *cis* (**2**)

Fig. 1. MESP of the α-aryl nitrone (**1**) and methacrolein *cis* (**2**)

Table 3. Local properties of dipole and dipolarophile calculated at B3LYP/6-31G(d) level of theory

Atoms	f^+	f^-	ω_k	N_k
O1	0.0037	0.9788	0.0061	3.2986
C3	0.5415	0.0001	0.8935	0.0003
C4	0.0000	0.0001	0.0000	0.0002
C5	0.0094	0.0016	0.0165	0.0035

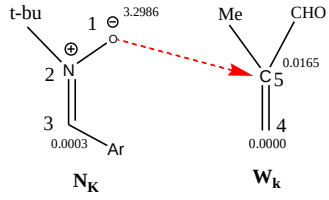

Fig. 2. Reactive scheme describes the preferred atomic centers for the interaction between dipole and dipolarophile

According to the values of local electrophilicity ω_k and local nucleophilicity N_k collected in Table 3, there are two most favorable interactions centers as described in Fig. 2. In our dipolar cycloaddition, the most favorable attack takes place between O1 atom of the dipole and C5 atom of the dipolarophile and between C3 atom of the dipole and C4 atom of the dipolarophile, respectively, leading to obtain the *meta*-regioisomer. This outcome is in full agreement with the experimental data earlier reported.

3.2. Mechanistic Study of the Cycloaddition Reaction Based on Activation Energy along the Different Paths of the Reaction

3.2.1. Mechanistic Study

The asymmetry of the investigated dipole and the dipolarophile (N-*tert*-butyl,α-(4-trifluoromethyl)-phenylnitrone (**1**) and methacrolein (**2**) (*cis*/*trans*) conducts to diverse reaction channels including two regioisomeric channels *ortho* and *meta* and the two stereoisomeric approaches *endo* and *exo*.

In the studied 32CA, there are sixteen possible transition states: Eight TSs for cyclization mode A (CM-A) could be formed by the reaction of the N-*tert*-butyl,α-(4-trifuoromethyl)-phenylnitrone (**1**) with methacrolein (**2**) *cis* namely TS1n-SS-c, TS1n-RR-c, TS1x-RS-c, TS1x-SR-c, TS2n-RR-c, TS2n-SS-c, TS2x-RSc, and TS2x-SR-c. Their corresponding isoxazolidines cycloadducts are CA1n-SS-c, CA1n-RR-c, CA1x-RS-c, CA1x-SR-c, CA2n-RRc, CA2n-SS-c, CA2x-RS-c and CA2x-SR-c, (Scheme 4). Besides, eight TSs for cyclization mode B (CM-B) could be obtained by the reaction of the N-*tert*-butyl,α-(4-trifuoromethyl)-phenylnitrone (**1**) with methacrolein (**2**) *trans* designated as TS1n-SS-t, TS1n-RR-t, TS1x-RS-t, TS1x-SR-t, TS2n-RR-t, TS2n-SS-t, TS2x-RS-t and TS2x-SR-t and their corresponding isoxazolidines cycloadducts CA1n-SS-t, CA1n-RR-t, CA1x-RS-t, CA1x-SR-t, CA2n-RR-t, CA2n-SS-t, CA2x-RS-t and CA2x-SR-t, (Scheme 5). The geometries of the previous sixteen TSs and their cycloadducts are confirmed by the presence of a single imaginary frequency.

Obviously, for each couple of enantiomers, the same bond lengths for the two forming sigma bonds are identical as represented in Fig. 3 and Fig. 4. The studied kinetic and thermodynamic of all the stationary points in DCM solvent are summarized in Table 4. The diagram of enthalpy profiles for the examined reaction paths associated with the 32CA of transition structures and products of the sixteen studied reactions in aqueous phase (DCM) are given in Fig. 5.

Analysis of the activation enthalpies listed in Table 4 along the reaction channels allows drawing some appealing conclusions. The activation enthalpy corresponding to TS1n-SS-c, and TS1n-RR-c shows the lowest activation enthalpy (13.05 kcal mol^{-1}) compared to that of the other TSs. The enthalpy differences between TS1n-SS-c/TS1n-RR-c and the other couples of enantiomers are 5.5 kcal mol^{-1} for TS1x-RS-c/TS1x-SR-c, 2.21 kcal mol^{-1} for TS2n-SS-c/TS2n-RR-c and 6.16 kcal $mol^{-1}$for TS2x-RSc/TS2x-SR-c.

For the CM-B, the most favorable reaction pathway corresponds to the formation of the *endo* CA1n-SS-t and CA1n-RR-t cycloadducts, *via* TS1n-SS-t and TS1n-RR-t, respectively. For the CM-B, the activation enthalpy of TS1n-SS-t and TS1n-RR-t TSs is 16.61 kcal mol^{-1} above the reagents in dichloromethane. The activation enthalpy difference between TS1n-SS-t/TS1n-RR-t and the other couples of enantiomers are 2.65 kcal mol^{-1} for TS1x-RS-t/TS1x-SR-t, 2.25 kcal mol^{-1} for TS2n- SS-t/TS2n-RR-t and 4.1 kcal mol^{-1} for TS2x-RS-t/TS2x-SR-t.

The strong exothermic character of these reactions makes them irreversible. Concerning the stability of the products CA1n-SS-c/CA1n-RR-c and CA1x-SR-c /CA1x-RS-c, we found a difference of 6.87 kcal mol^{-1} in favor of the formation of CA1n-SS-c/ CA1n-RR-c cycloadduct, that is to say, the formation of pathways CA1n-SS-c/CA1n-RR-c is easier than CA1x-SR-c/CA1x-RS-c.

The inclusion of entropies to enthalpies increases the activation Gibbs free energies where the calculated Gibbs free energies show that all the studied reaction paths are exergonic. Nevertheless, *meta-cis* approach (TS1n-SS-c/TS1n-RR-c isomers) is predicted to be the most thermodynamically favored cycloadduct although the difference, in Gibbs free energy, between the other approaches is very small, which is in good agreement with experimental findings.[24]

3.2.2. Geometries of the Transition Structures and Wiberg Bond Orders Analysis

Table 5 lists the bond distances (in Å) and (l) indices of the two newly formed bonds at the transition structures calculated in DCM are at DFT/B3LYP / 6-31(d). At the TSs associated with the *meta* reaction channel *via* CM-A, the bond length of the O1–C5 and C3–C4 are 2.40 and 2.00 Å for TS1n-SS-c/TS1n-RR-c, respectively, and 2.40 and 2.00 Å for TS1x-SR-c/TS1x-RS-c, respectively. Also, at the TSs associated to the *ortho* reaction channel *via* CM-A, we can see for both transition structures TS2n-SS-c/TS2n-RR-c and TS2x-SR-c/TS2x-RS-c, the lengths of the bonds of the O1–C4 are 1.65 and 1.67 Å, and C3–C5 2.54 and 2.52 Å; and we can see the stage of advancement C3–C4 sigma bond increases (I), while for the C5–O1 sigma bond the stage of advancement is reduced (I), for all TSs associated with *meta-endo* reaction channel *via* CM-A and CM-B, while we see the opposite for all TSs associated with the *ortho-endo* reaction channel *via* CM-A and CM-B where the stage of advancement C4–O1 sigma bond increases (I), while for the C5–C3 sigma bond the stage of advancement is reduced (I).

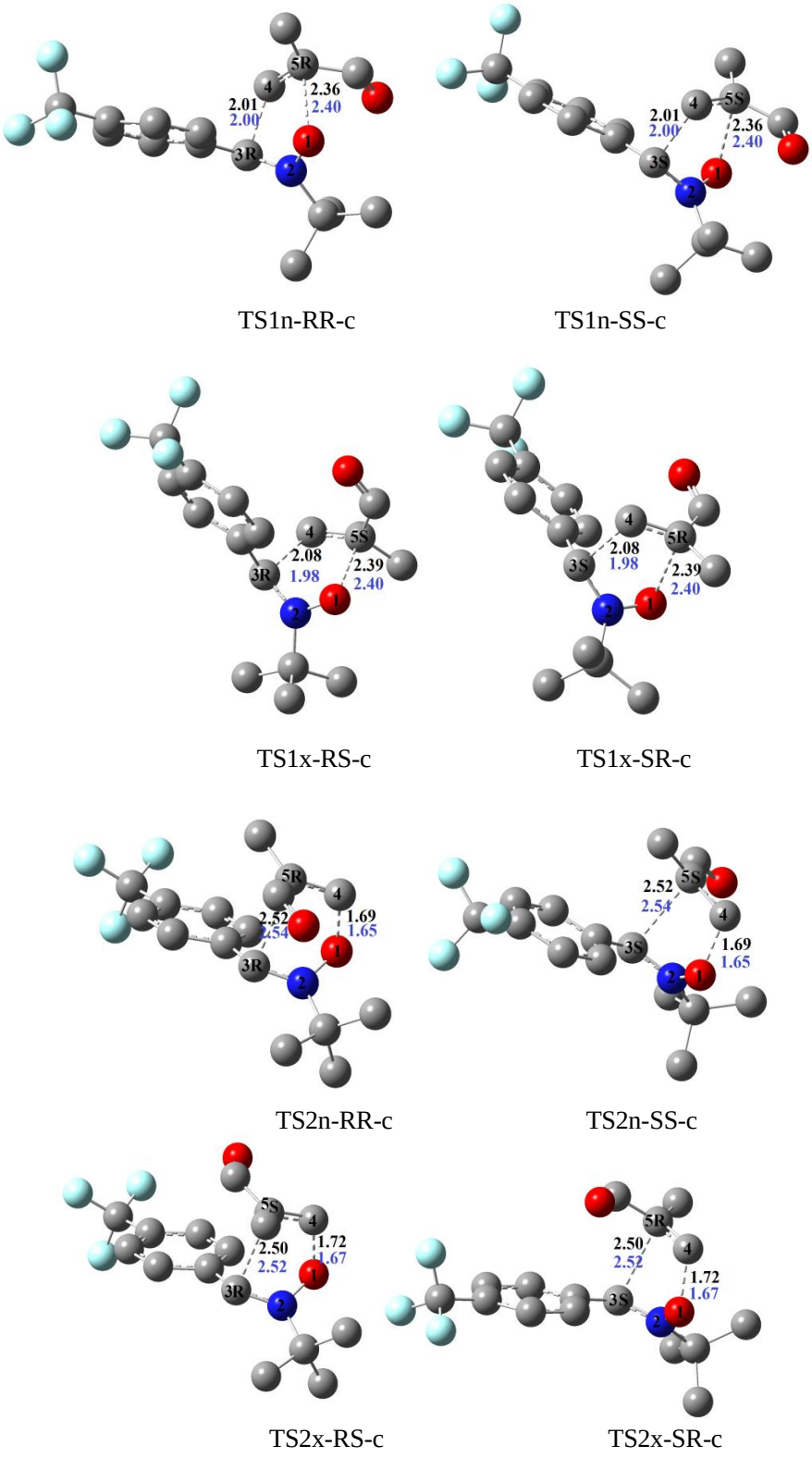

Fig. 3. B3LYP/6-31G(d) geometries of the transition structures involved in the 32CA reaction between the α-aryl nitrone (**1**) and methacrolein (**2**) *cis via* CM-A including the lengths of the new forming bonds in Angstroms

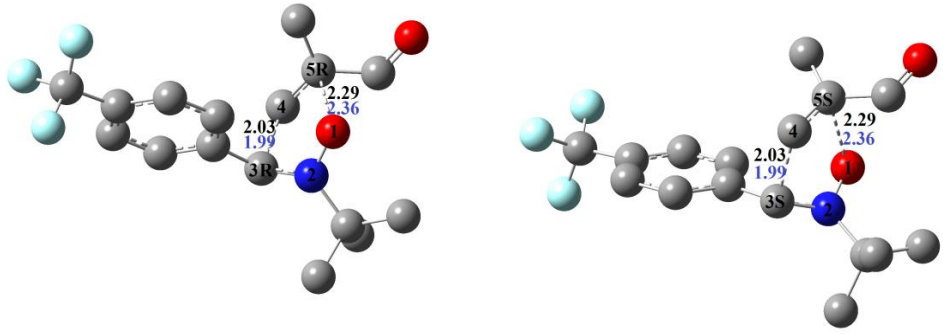

TS1n-RR-t

TS1n-SS-t

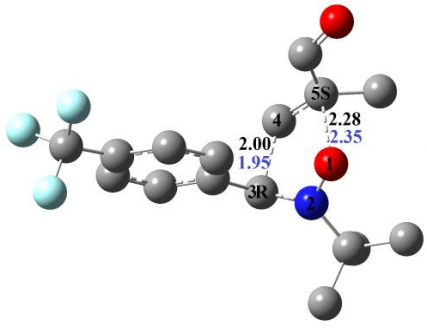

TS1x-RS-t

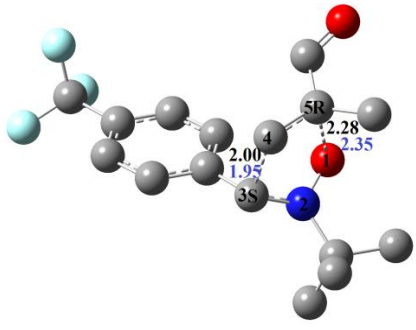

TS1x-SR-t

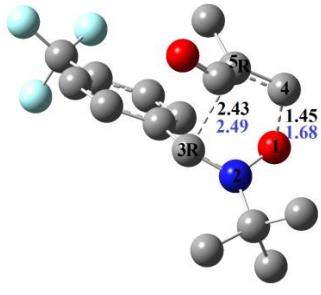

TS2n-RR-t

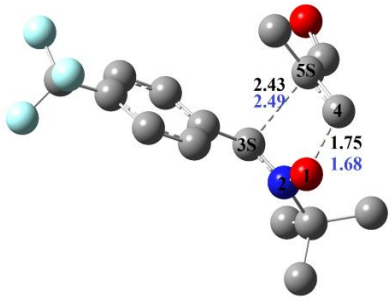

TS2n-SS-t

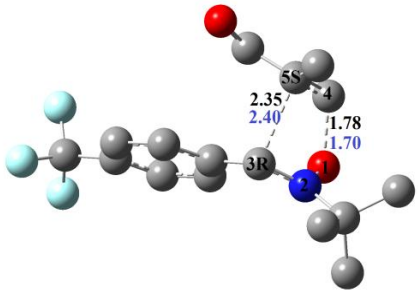

TS2x-RS-t

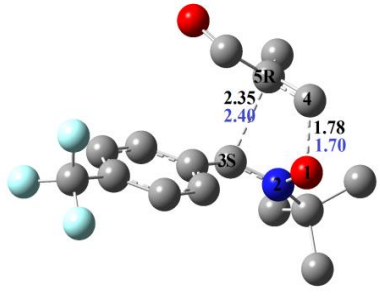

TS2x-SR-t

Fig. 4. B3LYP/6-31G(d) geometries of the transition structures involved in the 32CA reaction between the α-aryl nitrone (**1**) and methacrolein (**2**) *trans via* CM-B including the lengths of the new forming bonds in Angstroms

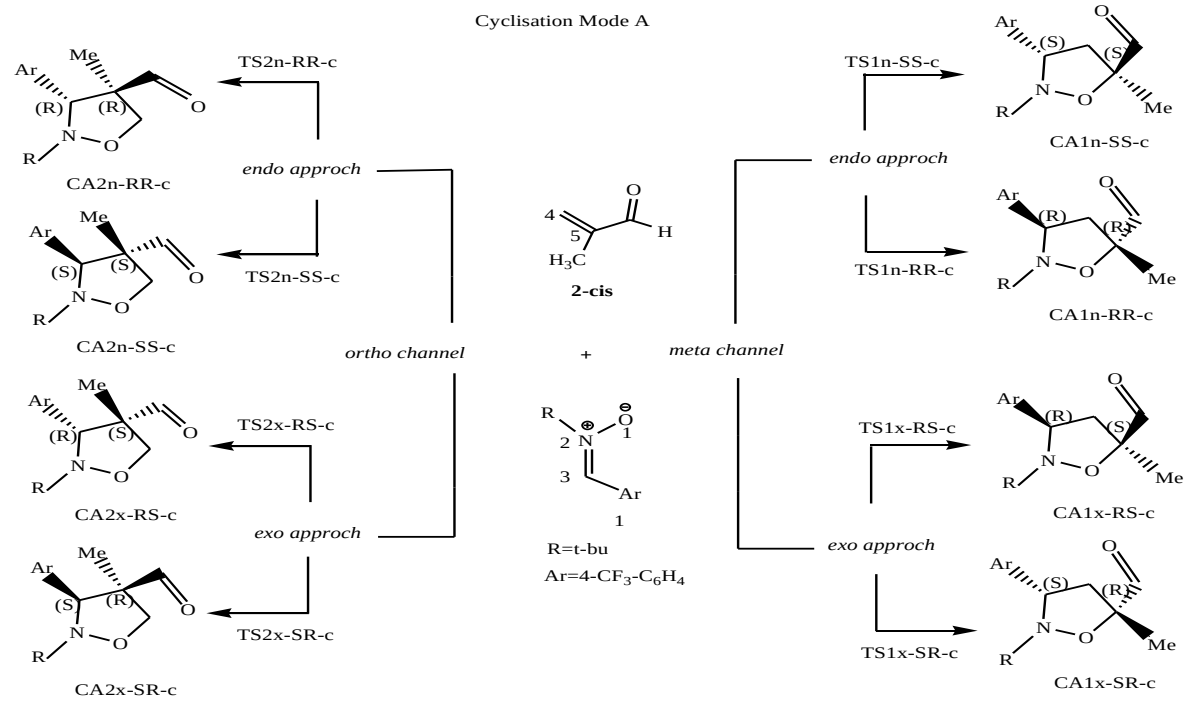

Scheme. 4. Regio- and stereoisomeric channels corresponding to the 32CA reaction of α-aryl nitrone (**1**) with methacrolein (**2**) *cis*

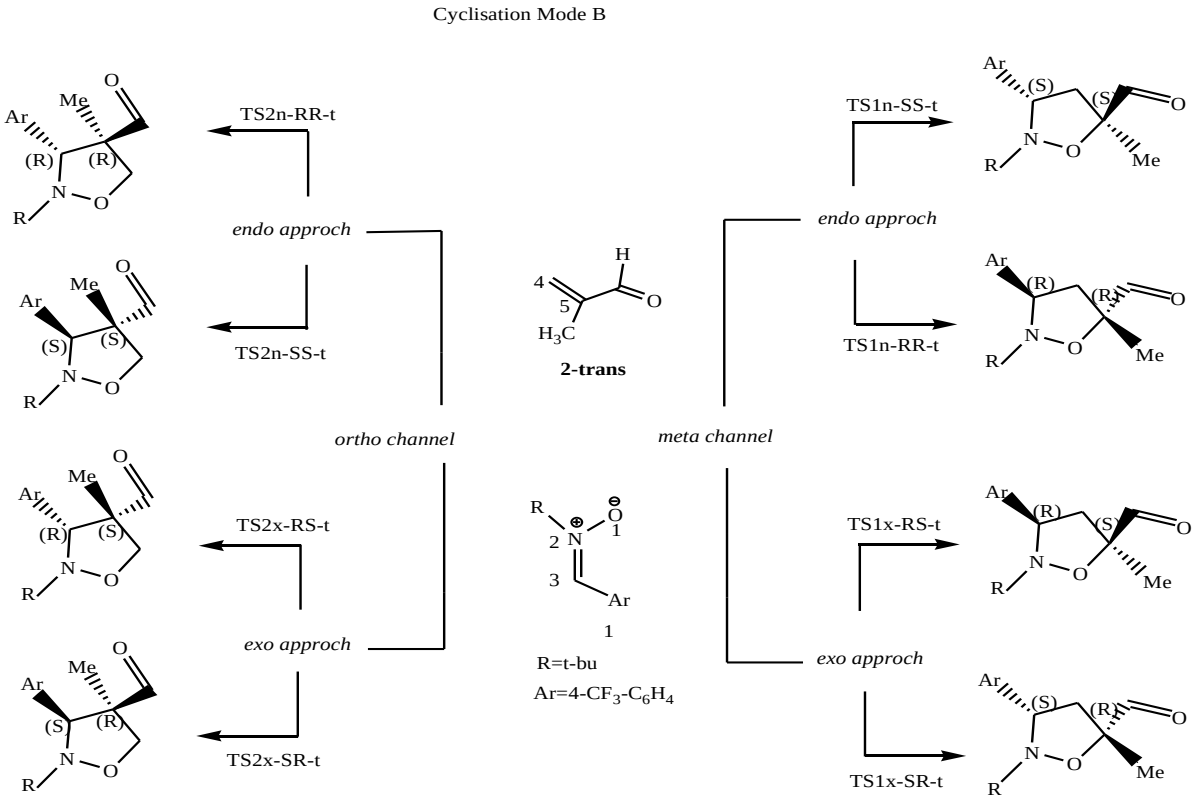

Scheme. 5. Regio-and stereoisomeric channels corresponding to the 32CA reaction of α-aryl nitrone (**1**) with methacrolein (**2**) *trans*

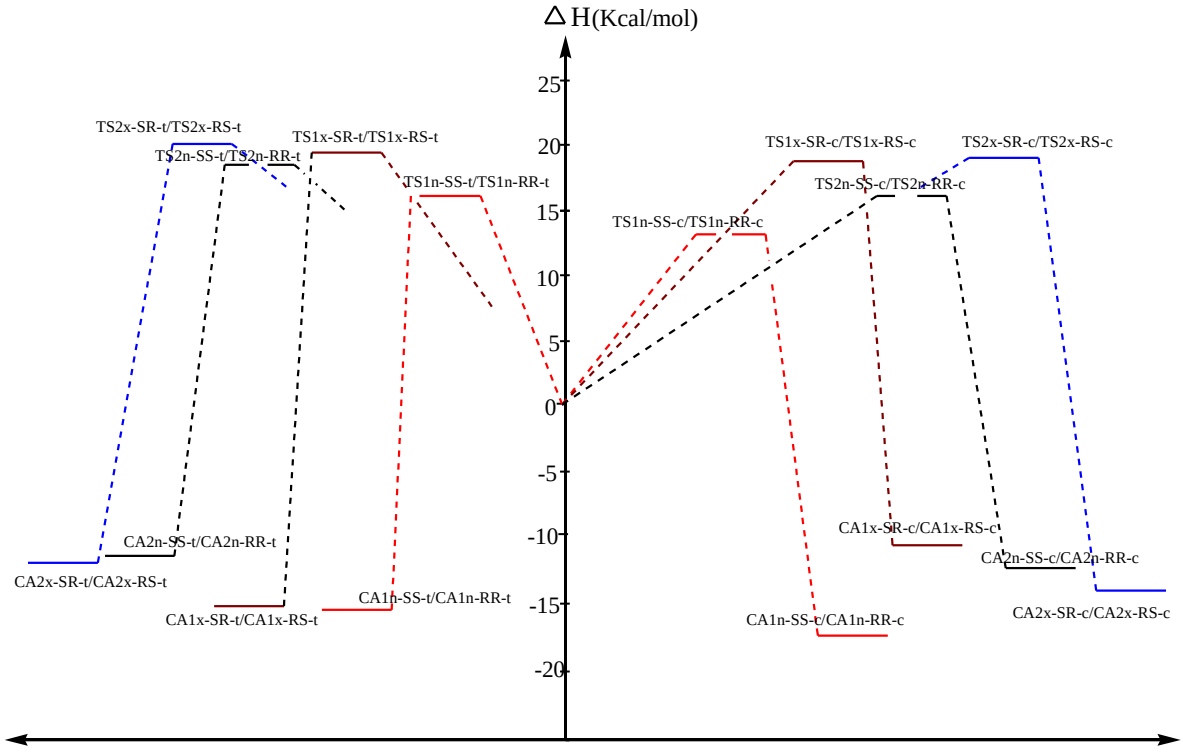

Fig. 5. Enthalpy profiles, in kcal mol^{-1}, for the examined reaction paths associated with the 32CA of transition structures and products of the sixteen studied reactions in aqueous phase (DCM)

Table 4. Kinetic and thermodynamic data for the 32CA reaction of the α-aryl nitrone (**1**) and methacrolein (**2**) *cis*/*trans* calculated at MPW1PW91/6-31G(d) in DCM at 298 K

	Dichloromethane						
	E	ΔE [a]	*H*	ΔH [a]	*G*	ΔG [a]	ΔS [a]
1	2	3	4	5	6	7	8
Cyclization mode A							
1	-895.167859		-894.700428		-894.760661		
2-*cis*	-231.233168		-231.073467		-231.109112		
TS1n-SS-c	-1126.377276	14.90	-1125.753101	13.05	-1125.827531	26. 51	-45.15
TS1n-RR-c	-1126.377276	14.90	-1125.753101	13.05	-1125.827531	26. 51	-45.15
TS1x-SR-c	-1126.368698	20.29	-1125.744327	18.55	-1125.819667	31.44	-43.23
TS1x-RS-c	-1126.368698	20.29	-1125.744327	18.55	-1125.819666	31.44	-43.23
TS2n-SS-c	-1126.373100	17.52	-1125.749571	15.26	-1125.823903	28.78	-45.35
TS2n-RR-c	-1126.373100	17.52	-1125.749570	15.26	-1125.823900	28.78	-45.35
TS2x-SR-c	-1126.366837	21. 45	-1125.743277	19. 21	-1125.817792	32.62	-44.98
TS2x-RS-c	-1126.366837	21. 45	-1125.743277	19. 21	-1125.817791	32.62	-44.98
CA1n-SS-c	-1126.419165	-11.38	-1125.801948	-17. 60	-1125.876956	-4. 51	-43.89
CA1n-RR-c	-1126.419165	-11.38	-1125.801948	-17. 60	-1125.876955	-4. 51	-43.89
CA1x-SR-c	-1126.408459	-4.52	-1125.790989	-10. 73	-1125.864926	3.04	-46.19
CA1x-SR-c	-1126.408459	-4.52	-1125.790989	-10. 73	-11..25.864926	3.04	-46.19
CA2n-SS-c	-1126.412386	-7.13	-1125.795607	-13. 62	-1125.869531	0.15	-46.19
CA2n-RR-c	-1126.412386	-7.13	-1125.795607	-13. 62	-1125.869532	0.15	-46.19
CA2x-SR-c	-1126.413411	-7.77	-1125.796606	-14. 25	-1125.869800	-0.02	-47.73
CA2x-RS-c	-1126.413411	-7.77	-1125.796605	-14. 25	-1125.869801	-0.02	-47.73
	Cyclization mode B						
1	-895.167859		-894.700428		-894.760661		
2-*trans*	-231.237866		-231.077941		-231.113149		

Continuation of Table 4

1	2	3	4	5	6	7	8
TS1n-SS-t	-1126.375502	18.97	-1125.751905	16.61	-1125.826701	29. 56	-43.44
TS1n-RR-t	-1126.375502	18.97	-1125.751905	16.61	-1125.826701	29. 56	-43.44
TS1x-SR-t	-1126.371071	21.75	-1125.747677	19.26	-1125.823424	31.62	-41.46
TS1x-RS-t	-1126.371071	21.75	-1125.747647	19.28	-1125.823471	31.59	-41.29
TS2n-SS-t	-1126.371171	21.68	-1125.748316	18.86	-1125.823348	31.67	-42.97
TS2n-RR-t	-1126.371171	21.68	-1125.748322	18.86	-1125.823347	31.67	-42.97
TS2x-SR-t	-1126.368151	23.58	-1125.745366	20.71	-1125.820753	33.29	-42.19
TS2x-RS-t	-1126.368151	23.58	-1125.745366	20.71	-1125.820752	33.29	-42.19
CA1n-SS-t	-1126.421082	-9.64	-1125.803237	-15.61	-1125.878160	-2.73	-43.20
CA1n-RR-t	-1126.421082	-9.64	-1125.803237	-15.61	-1125.878160	-2.73	-43.20
CA1x-SR-t	-1126.420361	-9.18	-1125.802787	-15.32	-1125.876729	-1.83	-45.25
CA1x-RS-t	-1126.420359	-9.18	-1125.802787	-15.32	-1125.876549	-1.72	-45.62
CA2n-SS-t	-1126.414281	-5.37	-1125.797695	-12.13	-1125.871297	1.58	-46.89
CA2n-RR-t	-1126.414281	-5.37	-1125.797695	-12.13	-1125.871297	1.58	-46.89
CA2x-SR-t	-1126.414661	-5.61	-1125.797770	-12.18	-1125.870695	1.96	-47.43
CA2x-RS-t	-1126.414661	-5.61	-1125.797771	-12. 18	-1125.870695	1.96	-47.43

[a] Relative to reactants.

Table 5. Bond distances and bond differences (in Angstrom) of the two newly formed bonds at the transition structures

	DCM								
	Meta channels				*Ortho* channels				
	d(O1-C5)	I	d(C3-C4)	I		d(O1-C4)	I	d(C3-C5)	I
TS1n-SS-c CA1n-SS-c	2.40 1.46	0.36	2.00 1.55	0.71	TS2n-SS-c CA2n-SS-c	1.65 1.42	0.84	2.54 1.58	0.40
TS1n-RR-c CA1n-RR-c	2.40 1.46	0.36	2.00 1.55	0.71	TS2n-RR-c CA2n-RR-c	1.65 1.42	0.84	2.54 1.58	0.40
TS1x-SR-c CA1x-SR-c	2.40 1.47	0.37	1.98 1.54	0.71	TS2x-SR-c CA2x-SR-c	1.67 1.42	0.82	2.52 1.57	0.40
TS1x-RS-c CA1x-RS-c	2.40 1.47	0.37	1.98 1.54	0.71	TS2x-RS-c CA2x-RS-c	1.67 1.42	0.82	2.52 1.57	0.40
TS1n-SS-t CA1n-SS-t	2.36 1.43	0.35	1.99 1.55	0.72	TS2n-SS-t CA2n-SS-t	1.68 1.42	0.82	2.49 1.58	0.42
TS1n-RR-t CA1n-RR-t	2.36 1.43	0.35	1.99 1.55	0.72	TS2n-RR-t CA2n-RR-t	1.68 1.42	0.82	2.49 1.58	0.42
TS1x-SR-t CA1x-SR-t	2.35 1.42	0.35	1.95 1.56	0.75	TS2x-SR-t CA2x-SR-t	1.70 1.42	0.80	2.40 1.57	0.47
TS1x-RS-t CA1x-RS-t	2.35 1.42	0.35	1.95 1.56	0.75	TS2x-RS-t CA2x-RS-t	1.70 1.42	0.82	2.40 1.57	0.47

These values show a change of the asynchronicity on the bond formation process for the two newly formed bonds in these TSs. This study shows that the 32CA reaction takes place along a one-step non-concerted mechanism, involving asymmetric reagents. The values of the percentage of the new sigma bonds for the reaction between N-*tert*-butyl-(4-trifluoromethyl)-phenylnitrone (**1**) and methacrolein (*cis*/*trans*) for obtaining the *meta* channel in gas phase and DCM for O1-C5 are (25.21 %-32.83 %)/(23.35 %-36.44 %) while for C3-C4 the percentage varies between (46.63 % and 52.42 %)/(46.89 % and 56.82 %) so the evolution of the formation of C3-C4 bond is more advanced than O1-C5. Concerning the *ortho* channel, the reaction between N-*tert*-butyl-(4-trifluoromethyl)-phenylnitrone (**1**) and methacrolein (*cis*/*trans*), for O1-C4 we have found (62.79 %-70.04 %)/(68.39 %-73.61 %) and for C3-C5 (30.59 %-37.23 %)/(30.40 %-34.93 %); consequently, the O1-C4 is more advanced than C3-C5 and the process of the formation of the new sigma bonds in this case is more or less asynchronous. The more asynchronous transition state for a variety of 32CA has the lower energy; so thus, agreement with the fact the empirical rule.[49-52]

Table 6. Wiberg bond orders of forming bonds at transition structures and cycloadducts and percentage of their formation at TSs. b3lyp/6-31G(d)

Cyclization mode A						
Gas phase				Dichloromethane		
Meta channels	d(O1-C5)	d(C3-C4)		d(O1-C5)	d(C3-C4)	
	TS P	TS P		TS P	TS P	
1n-SS-c	0.2178 0.8640	0.4917 0.9685	1n-SS-c	0.2011 0.8614	0.4967 0.9687	
	25. 21	50.77		23. 35	51. 27	
1n-RR-c	0.2178 0.8640	0.4918 0.9685	1n-RR-c	0.2011 0.8614	0.4967 0.9687	
	25.21	50.78		23. 35	51. 28	
1x-SR-c	0.1890 0.8607	0.4455 0.9792	1x-SR-c	0.1851 0.8617	0.4488 0.9799	
	32.83	46.63		32.34	46.89	
1x-RS-c	0.1890 0.8606	0.4456 0.9792	1x-RS-c	0.1851 0.8617	0.4488 0.9799	
	32.83	46.63		32.34	46.89	
Ortho channels	d(O1-C4)	d(C3-C5)		d(O1-C4)	d(C3-C5)	
2n-SS-c	0.6198 0.9195	0.2354 0.9295	2n-SS-c	0.6552 0.9191	0.2356 0.9316	
	70.03	30.59		73.61	30.40	
2n-RR-c	0.6198 0.9294	0.2354 0.9294	2n-RR-c	0.6552 0.9192	0.2356 0.9316	
	70.04	30.60		76.60	30.40	
2x-SR-c	0.5926 0.9235	0.2558 0.9417	2x-SR-c	0.6407 0.9165	0.2573 0.9381	
	66.91	31.41		72.42	31.92	
2x-RS-c	0.5925 0.9235	0.2557 0.9417	2x-RS-c	0.6407 0.9166	0.2573 0.9381	
	66.91	31.40		72.42	31.92	
Cyclization mode B						
Gas phase				Dichloromethane		
Meta channels	d(O1-C5)	d(C3-C4)		d(O1-C5)	d(C3-C4)	
	TS P	TS P		TS P	TS P	
1n-SS-t	0.2487 0.8967	0.4784 0.9712	1n-SS-t	0.2207 0.8944	0.5028 0.9716	
	27.74	49.26		24. 68	51.75	
1n-RR-t	0.2488 0.8967	0.4784 0.9712	1n-RR-t	0.2207 0.8944	0.5028 0.9716	
	27.75	49.26		24. 68	51.75	
1x-SR-t	0.2833 0.9142	0.5098 0.9726	1x-SR-t	0.2732 0.9088	0.5407 0.9725	
	30.99	52.42		36.44	56.82	
1x-RS-t	0.2833 0.9142	0.5097 0.9726	1x-RS-t	0.2732 0.9088	0.5407 0.9725	
	30.99	52.41		36.44	56.82	
ortho channels	d(O1-C4)	d(C3-C5)		d(O1-C4)	d(C3-C5)	
2n-SS-t	0.5749 0.9240	0.2802 0.9302	2n-SS-t	0.6267 0.9171	0.2542 0.9296	
	65.09	35		70.96	32.46	
2n-RR-t	0.5749 0.9239	0.2802 0.9303	2n-RR-t	0.6266 0.9171	0.2742 0.9296	
	65.10	34.99		70.95	32.46	
2x-SR-t	0.5545 0.9266	0.3060 0.9337	2x-SR-t	0.6096 0.9257	0.2814 0.9321	
	62.79	37.23		68.39	34.93	
2x-RS-t	0.5545 0.9266	0.3060 0.9337	2x-RS-t	0.6096 0.9257	0.2814 0.9321	
	62.79	37.23		68.39	34.93	

3.2.3. Study of Charge Transfer in TSs

Natural bond orbital (NBO) analysis allows us to evaluate the charge transfer (CT) along with the cycloaddition processes. For 32CA reactions between nucleophilic and the electrophilic structures for the precedent reactions, the evaluation of the electronic nature showed that the atomic charges in the TSs were shared between the α-aryl nitrone (**1**) and methacrolein (**2**) *cis*/*trans*.

Positive values in the gas and solvent phases are indicative of an electron flow from the α-aryl nitrone (**1**) and methacrolein (**2**) *cis* for all the eight TSs for CM-A, ranges from 0.04 to 0.128e, indicating the polar nature of the 32CA reactions as it can be seen in Tables 2 and 7.

The global electronic density transfer (GEDT) values are found to be lower for all TSs under study for CM-B, ranges from 0.04 to 0.09 e, which reveals that these 32CA reactions have a moderate polar character as a consequence of the moderate nucleophilic character of dipoles.

Table 7. The charge transfer (CT) in TSs at B3LYP/6-31G(d)

Cyclization mode A	CT		Cyclization mode B	CT	
	Gas phase	DCM		Gas phase	DCM
TS1n-SS-c	0.080	0.104	TS1n-SS-t	0.049	0.092
TS1n-RR-c	0.080	0.104	TS1n-RR-t	0.049	0.092
TS1x-SR-c	0.043	0.091	TS1x-SR-t	0.047	0.093
TS1x-RS-c	0.043	0.091	TS1x-RS-t	0.047	0.093
TS2n-SS-c	0.092	0.127	TS2n-SS-t	0.045	0.093
TS2n-RR-c	0.093	0.128	TS2n-RR-t	0.045	0.093
TS2x-SR-c	0.084	0.128	TS2x-SR-t	0.046	0.090
TS2x-RS-c	0.085	0.128	TS2x-RS-t	0.046	0.090

4. Conclusions

In this computational study, the mechanism and the regio- and diastereo-selectivity of the 32CA reactions between N-*tert*-butyl,α-(4-trifluoromethyl)-phenylnitrone (**1**) and methacrolein (**2**) *cis*/*trans* have been studied in detail using the density functional theory (DFT) calculations at B3LYP/6-31G(d) level in gas and DCM media. In the light of the above discussions, it was concluded that:

- The global and local indices of reactants revealed that N-*tert*-butyl,α-(4-trifluoromethyl)-phenylnitrone (**1**) acts as a nucleophile and methacrolein (**2**) is considered as an electrophile in the studied reaction.
- The analysis of electronic chemical potentials indicates a normal electron demand character for the investigated reaction.
- DFT results show that the *meta-endo* reaction channel *via* CM-A, yielding the (3R,5R) and (3S,5S) *endo* cycloadducts are the preferred pathway in the studied process.
- The geometrical parameters and Wiberg bond indices indicate that the examined cycloaddition reaction follows a one-step non-concerted mechanism and is asynchronous in the formation of the two new sigma bonds.

Acknowledgement

The authors would like to thank Prof. Abdelmalek Khorief Nacereddine, member in the laboratory of organic synthesis and catalysis, department of chemistry, Annaba, Algeria for his beneficial advices and scientific skills.

References

[1] Padwa, A. *1,3-Dipolar Cycloaddition Chemistry*; Wiley-Interscience: New York, 1984.
[2] Gothelf, K.V., Jorgensen, K.A. Asymmetric 1,3-Dipolar Cycloaddition Reactions. *Chem. Rev*. **1998**, *98*, 863-910. http://doi.org/10.1021/cr970324e
[3] Jasiński, R. A New Insight on the Molecular Mechanism of the Reaction between (Z)-C,N-Diphenylnitrone and 1,2-Bismethylene-3,3,4,4,5,5-hexamethylcyclopentane. *J. Mol. Graph. Model*. **2020**, *94*, 107461. http://doi.org/10.1016/j.jmgm.2019.107461
[4] Jasiński, R. Competition between One-Step and Two-Step Mechanism in Polar [3 + 2] Cycloadditions of (Z)-C-(3,4,5-Trimethoxyphenyl)-N-methyl-nitrone with (Z)-2-EWG-1-Bromo-1-nitroethenes. *Comput. Theor. Chem*. **2018**, *1125*, 77-85. https://doi.org/10.1016/j.comptc.2018.01.009
[5] Jasiński, R. Nitroacetylene as Dipolarophile in [2 + 3] Cycloaddition Reactions with Allenyl-Type Three-Atom Components: DFT Computational Study. *Monatsh. Chem*. **2015**, *146*, 591-599. https://doi.org/10.1007/s00706-014-1389-0
[6] Jasiński, R.; Jasińska, E.; Dresler, E. A DFT Computational Study of the Molecular Mechanism of [3 + 2] Cycloaddition Reactions between Nitroethene and Benzonitrile N-Oxides. *J. Mol. Model*. **2017**, *23*, 13. https://doi.org/10.1007/s00894-016-3185-8
[7] Jasiński, R. Competition between the One-Step and Two-Step, Zwitterionic Mechanisms in the [2+3] Cycloaddition of Gem-Dinitroethene with (Z)-C,N-Diphenylnitrone: A DFT Computational Study. *Tetrahedron* **2013**, *69*, 927-932. https://doi.org/10.1016/j.tet.2012.10.095
[8] Padwa, A. *Synthetic Applications of 1,3-Dipolar Cycloaddition Chemistry Towards Heterocycles and Natural Products*; Wiley and Sons: Hoboken, 2003.
[9] Merino, P. In *Science of Synthesis*, Vol. 27; Padwa, A., Ed.; George Thieme: New York, 2004.
[10] Jones, G.O.; Houk, K.N. Predictions of Substituent Effects in Thermal Azide 1,3-Dipolar Cycloadditions: Implications for Dynamic Combinatorial (Reversible) and Click (Irreversible) Chemistry. *J. Org. Chem*. **2008**, *73*, 1333-1342. https://doi.org/10.1021/jo702295d
[11] Parr, R.G.; Pearson R.G. Absolute Hardness: Companion Parameter to Absolute Electronegativity. *J. Am. Chem. Soc*. **1983**, *105*, 7512-7516. https://doi.org/10.1021/ja00364a005
[12] Minter, A.R.;, Brennan, B.B.; Mapp, A.K. A Small Molecule Transcriptional Activation Domain. *J. Am. Chem. Soc*. **2004**, *126*, 10504-10505. https://doi.org/10.1021/ja0473889
[13] Chiacchio, U.; Rescifina, A.; Iannazzo, D.; Piperno, A.; Romeo, R.; Borrello, L.; Sciortino, M.T.; Balestrieri, E.; Macchi, B.; Mastino, A. et al. Phosphonated Carbocyclic 2‘-Oxa-3‘-azanucleosides as New Antiretroviral Agents. *J. Med. Chem*. **2007**, *50*, 3747-3750. https://doi.org/10.1021/jm070285r
[14] Ding, P.; Miller, M.; Chen, Y.; Helquist, P.; Oliver, A.J.; Wiest, O. Syntheses of Conformationally Constricted Molecules as Potential NAALADase/PSMA Inhibitors. *Org. Lett*. **2004**, *6*, 1805-1808. https://doi.org/10.1021/ol049473r
[15] Wess, G., Kramer, W., Schuber, G.; Enhsen, A.; Baringhaus, K.-H.; Glombik, H.; Müllner, S.; Bock, K.; Kleine, H.; John, M. et al. Synthesis of Bile Acid – Drug Conjugates: Potential Drug – Shuttles for Liver Specific Targeting. *Tetrahedron. Lett*. **1993**, *34*, 819-822. https://doi.org/10.1016/0040-4039(93)89021-H

[16] Merino, P.; Tejero, T.; Unzurrunzaga, F.J.; Franco, S.; Chiacchio, U.; Saita, M.G.; Iannazzo, D.; Piperno, A.; Romeo, G. An Efficient Approach to Enantiomeric Isoxazolidinyl Analogues of Tiazofurin Based on Nitrone Cycloadditions. *Tetrahedron Asymmetry* **2005**, *16*, 3865-3876. https://doi.org/10.1016/j.tetasy.2005.11.004
[17] Mannucci, V.; Cordero, F.M.; Piperno, A.; Romeo, G.; Brandi, A. Diastereoselective Synthesis of a Collection of New Homonucleoside Mimetics Containing Pyrrolo[1,2-b]isoxazoline and Pyrrolidine Rings. *Tetrahedron Asymmetry* **2008**, *19*, 1204-1209. https://doi.org/10.1016/j.tetasy.2008.04.028
[18] Romeo, R.; Giofre, S.V.; Macchi, B.; Balestrieri, E.; Mastino, A.; Merino, P.; Carnovale, C.; Romeo, G.; Chiacchio, U. Truncated Reverse Isoxazolidinyl Nucleosides: A New Class of Allosteric HIV-1 Reverse Transcriptase Inhibitors. *ChemMedChem*. **2012**, *7*, 565-569. https://doi.org/10.1002/cmdc.201200022
[19] Kiguchi, T.; Shirakawa, M.; Honda, R.; Ninomiya, I.; Naito, T. Total Synthesis of (+)-Azimic Acid, (+)-Julifloridine, and Proposed Structure of N-Methyljulifloridine *via* Cycloaddition of Nitrone to a Chiral Dipolarophile. *Tetrahedron* **1998**, *54*, 15589-15606. https://doi.org/10.1016/S0040-4020(98)01012-6
[20] Cardona, F.; Moreno, G.; Guarna, F.; Vogel, P.; Schuetz, C.; Merino, P.; Goti, A. New Concise Total Synthesis of (+)-Lentiginosine and Some Structural Analogues. *J. Org. Chem*. **2005**, *70*, 6552-6555. https://doi.org/10.1021/jo0509408
[21] Delso, I.; Tejero, T.; Goti, A.; Merino, P. Synthesis of d-Arabinose-Derived Polyhydroxylated Pyrrolidine, Indolizidine and Pyrrolizidine Alkaloids. Total Synthesis of Hyacinthacine A_2. *Tetrahedron* **2010**, *66*, 1220-1227. https://doi.org/10.1016/j.tet.2009.12.030
[22] Peng, J.; Jiang, D.; Lin, W.; Chen, Y. Palladium-Catalyzed Sequential One-Pot Reaction of Aryl Bromides with O-Homoallylhydroxylamines: Synthesis of N-Aryl-β-amino Alcohols. *Org. Biomol. Chem*. **2007**, *5*, 1391-1396. https://doi.org/10.1039/B701509G
[23] Andrade, M.; Barros, M.T.; Pinto, R.C. Clean and Sustainable Methodologies for the Synthesis of Isoxazolidines. In *Heterocyclic Targets in Advanced Organic Synthesis*; Carreiras, M. C.; Marco-Contelles, J., Eds.; Research Signpost: Trivandrum, India, 2011; pp 51-67.
[24] Bădoiu, A.; Kündig, E.P. Electronic Effects in 1,3-Dipolar Cycloaddition Reactions of N-Alkyl and N-Benzyl Nitrones with Dipolarophiles. *Org. Biomol. Chem*. **2012**, *10*, 114-121. https://doi.org/10.1039/C1OB06144E
[25] Frisch, M.J., Trucks, G.W., Schlegel, H.B. Gaussian 09, Revision D.01, CT 2009.
[26] Jasiński, R.; Koifman, O.I.; Barański, A. A DFT Study on the Regioselectivity and Molecular Mechanism of Nitroethene [2 + 3] Cycloaddition to (Z)-C,N-Diphenylnitrone and C,C,N-Triphenylnitrone. *Mendeleev Commun.* **2011**, *21*, 262-263. https://doi.org/10.1016/j.mencom.2011.09.010
[27] Domingo, L. R.; Ríos-Gutiérrez, M.; Pérez, P. A DFT Study of the Ionic [2+2] Cycloaddition Reactions of Keteniminium Cations with Terminal Acetylenes. *Tetrahedron* **2015**, *71*, 2421-2427. https://doi.org/10.1016/j.tet.2015.02.070
[28] Tirado-Rives, J.; Jorgensen, W.L. Performance of B3LYP Density Functional Methods for a Large Set of Organic Molecules. *J. Chem. Theory Comput*. **2008**, *4*, 297-306. https://doi.org/10.1021/ct700248k
[29] Cances, E.; Mennucci, B.; Tomasi, J. A New Integral Equation Formalism for the Polarizable Continuum Model: Theoretical Background and Applications to Isotropic and Anisotropic Dielectrics. *J. Chem. Phys*. **1997**, *107*, 3032. https://doi.org/10.1063/1.474659
[30] Cossi, M.; Barone, V.; Cammi, R.; Tomasi, J. Ab Initio Study of Solvated Molecules: A New Implementation of the Polarizable Continuum Model. *Chem. Phys. Lett*. **1996**, *255*, 327-335. https://doi.org/10.1016/0009-2614(96)00349-1
[31] Barone, V.; Cossi, M.; Tomasi, J. Geometry Optimization of Molecular Structures in Solution by the Polarizable Continuum Model. *J. Comput. Chem*. **1998**, *19*, 404-417. https://doi.org/10.1002/(SICI)1096-987X(199803)19:4<404::AID-JCC3>3.0.CO;2-W
[32] Domingo, L.R. A New C–C Bond Formation Model Based on the Quantum Chemical Topology of Electron Density. *RSC Adv*. **2014**, *4*, 32415-32428. https://doi.org/10.1039/C4RA04280H
[33] Mayer, I. Bond Orders and Valences from ab Initio Wave Functions. *Int. J. Quantum. Chem*. **1986**, *29*, 477-483. https://doi.org/10.1002/qua.560290320
[34] Keresztury, G.; Holly, S.; Besenyei, G.; Varga, J.; Wang, A.; Durig, J.R. Vibrational Spectra of Monothiocarbamates-II. IR and Raman Spectra, Vibrational Assignment, Conformational Analysis and AB Initio Calculations of S-Methyl-N,N-dimethylthiocarbamate. *Spectrochimica Acta Part A: Molecular Spectroscopy*. **1993**, *49*, 2007-2017, 2019-2026. https://doi.org/10.1016/S0584-8539(09)91012-1
[35] Reed, A.E.; Curtiss, L.A.; Weinhold, F. Intermolecular Interactions from a Natural Bond Orbital, Donor-Acceptor Viewpoint. *Chem. Rev*. **1988**, *88*, 899-926. https://doi.org/10.1021/cr00088a005
[36] Reed, A.E.; Weinstock, R.B.; Weinhold, F. Natural Population Analysis. *J. Chem. Phys*. **1985**, *83*, 735. https://doi.org/10.1063/1.449486
[37] Zhao, Y.; Truhlar, D.G. Hybrid Meta Density Functional Theory Methods for Thermochemistry, Thermochemical Kinetics, and Noncovalent Interactions: The MPW1B95 and MPWB1K Models and Comparative Assessments for Hydrogen Bonding and van der Waals Interactions. *J. Phys. Chem*. **2004**, *108*, 6908-6918. https://doi.org/10.1021/jp048147q
[38] Fukui, K. Formulation of the Reaction Coordinate. *J. Phys. Chem*. **1970**, *74*, 4161-4163. https://doi.org/10.1021/j100717a029
[39] Parr, R.G.; von Szentpaly, L.; Liu, S. Electrophilicity Index. *J. Am. Chem. Soc*. **1999**, *121*, 1922-1924. https://doi.org/10.1021/ja983494x
[40] Parr, R.G.; Yang, W. In *Density Functional Theory of Atoms and Molecules*; Oxford University: New York, 1989.
[41] Domingo, L.R.; Chamorro, E.; Pérez, P. Understanding the Reactivity of Captodative Ethylenes in Polar Cycloaddition Reactions. A Theoretical Study. *J. Org. Chem*. **2008**, *73*, 4615-4624. https://doi.org/10.1021/jo800572a
[42] Yang, W.; Mortier, W.J. The Use of Global and Local Molecular Parameters for the Analysis of the Gas-Phase Basicity of Amines. *J. Am. Chem. Soc*. **1986**, *108*, 5708-5711. https://doi.org/10.1021/ja00279a008
[43] Domingo, L.R.; Aurell, M.J.; Pérez, P.; Contreras, R. Quantitative Characterization of the Local Electrophilicity of Organic Molecules. Understanding the Regioselectivity on Diels−Alder Reactions. *J. Phys. Chem*. **2002**, *106*, 6871-6875. https://doi.org/10.1021/jp020715j
[44] Pérez, P.; Domingo, L.R.; Duque-Norna, M.; Chamorro, E. A Condensed-to-Atom Nucleophilicity Index. An Application to the Director Effects on the Electrophilic Aromatic Substitutions. J. *Mol. Struct. Theochem*. **2009**, *895*, 86-91. https://doi.org/10.1016/j.theochem.2008.10.014
[45] Mloston, G.; Jasinski, R.; Kula, K.; Heimgartner, H. A DFT Study on the Barton–Kellogg Reaction – The Molecular Mechanism of the Formation of Thiiranes in the Reaction between Diphenyldi-

azomethane and Diaryl Thioketones. *Eur. J. Org. Chem*. **2020**, *2020*, 176-182. https://doi.org/10.1002/ejoc.201901443
[46] Sustmann, R.; Shubert, R. Photoelektronenspektroskopische bestimmung von substituenten-effekten II. α,β-ungesättigte Carbonester. *Tetrahedron Lett.* **1972**, *13*, 4271-4274. https://doi.org/10.1016/S0040-4039(01)94292-3
[47] Šponer, J. Hobza, P. DNA Base Amino Groups and their Role in Molecular Interactions: Ab Initio and Preliminary Density Functional Theory Calculations. *Int. J. Quantum. Chem*. **1996**, *57*, 959-970. https://doi.org/10.1002/(SICI)1097-461X(1996)57:5<959::AID-QUA16>3.0.CO;2-S
[48] Murray, J.S.; Sen, K. *Molecular electrostatic potentials: concepts and 399 applications*; Elsevier: Amsterdam, 1996.
[49] Marakchi, K.; Kabbaj, O. K.; Komiha, N. Etude DFT du mécanisme des réactions de cycloaddition dipolaire-1,3 de la C,N-diphénylnitrone avec des dipolarophiles fluorés de type éthylénique et acétylénique. *J. Fluor. Chem*. **2002**, *114*, 81-89. https://doi.org/10.1016/S0022-1139(01)00570-X
[50] Marakchi, K.; Abou El Makarim, H.; Kabbaj, O. K.; Komiha, N. Etude Theorique du Mecanisme de la Reaction de Cycloaddition Dipolaire-1,3 du 3-Fluoro-3-Trifluoromethyl Prop-2-Enoate de Methyle Avec la Pyrroline-1-Oxyde. *Phys. Chem. News*. **2010**, *52*, 128-136.
[51] Marakchi, K.; Ghailane, R.; Kabbaj, O.K.; Komiha, N. DFT Study of the Mechanism and Stereoselectivity of the 1,3-Dipolar Cycloaddition between Pyrroline-1-oxide and Methyl Crotonate. *J. Chem. Sci*. **2014**, *126*, 283-292. https://doi.org/10.1007/s12039-013-0563-y
[52] Domingo, L.R. Theoretical Study of the 1,3-Dipolar Cycloaddition Reactions of Azomethine Ylides. A DFT Study of Reaction between Trifluoromethyl Thiomethyl Azomethine Ylide and Acrylonitrile. *J. Org. Chem*. **1999**, *64*, 3922-3929. https://doi.org/10.1021/jo9822683

Received: May 25, 2021 / Revised: June 17, 2021 / Accepted: July 05, 2021

[3+2] ЦИКЛОПРИЄДНАННЯ N-*трет*-БУТИЛ,α-(4-ТРИФЛУОРОМЕТИЛ)-ФЕНІЛНІТРОНУ З МЕТАКРОЛЕЇНОМ: ТЕОРЕТИЧНЕ ДОСЛІДЖЕННЯ

Анотація. *У цій роботі досліджено регіо- та діастереоселективність [3+2] циклоприєднання (32CA) N-трет-бутил,α-(4-трифлуорометил)-фенілнітрону (**1**) і метакролеїну (**2**) за допомогою методу DFT на B3LYP/6-31(d) обчислювальному рівні у газовій фазі та в розчиннику дихлорометані. Для виявлення найактивніших центрів у досліджуваних молекулах використовували молекулярний електростатичний потенціал MESP. Було розраховано глобальні і локальні показники реакційної здатності та термодинамічні параметри з метою пояснення регіоселективності та стереоселективності для обраної N-трет реакції. Досліджено можливу хемоселективну орто/мета регіоселективність та стерео- (ендо/екзо) ізомерні канали. Наші теоретичні результати дають важливе пояснення можливих шляхів, пов'язаних з досліджуваною реакцією 32CA.*

Ключові слова: *[3+2] циклоприєднання, N-трет-бутил,α-(4-трифлуорометил)-феніл, метакролеїн, DFT, регіоселективність, стереоселективність.*